

基于矢量分析的转子碰磨故障轴向定位方法

李录平, 邹新元, 晋风华

(长沙理工大学 能源与动力工程学院, 湖南 长沙 410076)

摘 要: 在对旋转机械转子碰磨振动行为进行研究的基础上, 对转子碰磨点轴向定位方法进行了探索, 提出了一种基于振动矢量分析的碰磨故障轴向定位方法。研究表明, 转轴表面与静子部分发生碰磨时, 转子会产生临时热弯曲, 从而引起转子的不平衡量发生变化。这种变化可通过转子两端的振动矢量的变化反映出来。利用转子两端的振动矢量的变化关系, 可以判断转子表面发生碰磨点的轴向位置。应用实例分析表明, 本文提出的旋转机械碰磨故障定位方法具有准确性。

关 键 词: 旋转机械; 碰磨; 故障定位

中图分类号: TK263. 6 文献标识码: A

1 前 言

大型旋转机械具有单机功率大、转速高、空间尺寸大、动静间隙小等特点, 在运转过程中, 热力状态的变化往往会导致动静间隙减小甚至消失, 从而引起动静碰磨。大型旋转机械一旦发生动静碰磨故障, 轻者使机组的效率降低, 重者引起机组剧烈振动, 甚至引起重大的设备事故。快速地诊断出机组的碰磨故障并准确确定碰磨的轴向位置, 是大型旋转机械故障诊断的重要内容。

文献[1~2]对旋转机械碰磨故障的机理和碰磨故障特征提取方法进行了较多的探讨, 但对旋转机械故障定位方法研究却鲜有报道, 特别是对碰磨故障定位方法的研究文献尚未出现。

大型旋转机械碰磨故障发生的部位不同, 其故障的原因差别很大, 故障引起的后果也不相同。因此, 在不同部位发生的碰磨故障, 采取的故障处理措施也不相同。所以, 实现对碰磨故障的快速定位具有重要的理论价值和工程应用价值。本文依据转子动力学的有关理论, 提出一种对大型旋转机械动静碰磨故障轴向定位的方法。本文所讨论的碰磨主要是指转子表面局部碰磨, 或全周碰磨情形中周向摩

擦不均匀导致局部弧段摩擦更加严重的情况。

2 旋转机械动静碰磨引起的转子热弯曲

设如图 1 所示的有阻尼单圆盘转子, 其振动方程为^[3~4]:

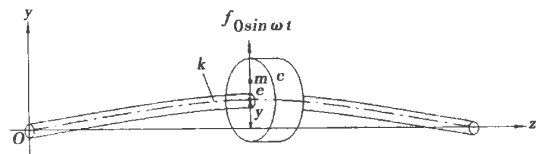


图 1 单圆盘转子模型

$$m \frac{d^2 y}{dt^2} + c \frac{dy}{dt} + ky = f_0 \sin \omega t \quad (1)$$

式(1)是一个二阶常系数线性非齐次微分方程, 其解由通解和特解组成:

$$y(t) = Ae^{-\zeta \omega_n t} \sin(\sqrt{1-\zeta^2} \omega_n t + \varphi) + B \sin(\omega t - \theta) \quad (2)$$

当系统具有一定的阻尼时, 上式右边第一项很快衰减为零, 只剩下第二项, 其中:

$$B = \frac{1}{\sqrt{(1-\gamma^2)^2 + 4\gamma^2 \zeta^2}} \times \frac{f_0}{k} = \beta \times y_{st} \quad (3)$$

$$\theta = \arctg \frac{2\zeta\gamma}{1-\gamma^2} \quad (4)$$

式(1)~式(4)中: m —转子的质量; c —阻尼系数; k —转子的弹性系数; ω_n —转子的固有频率(临界转速); $\gamma = \frac{\omega}{\omega_n}$ —频率比; $\zeta = \frac{c}{c_c} = \frac{c}{2\sqrt{km}}$ —阻尼比; $y_{st} = \frac{f_0}{k}$ —零频率偏移; β —动力放大因子; θ —机械滞后角(又称为相位角), 它是激振力与激振力引起的动挠度之间的夹角。

收稿日期: 2005-05-24; 修订日期: 2005-10-11

基金项目: 国家自然科学基金资助项目(50105004); 湖南省自然科学基金资助项目(01JJY3022)

作者简介: 李录平(1963-), 男, 湖南邵阳人, 长沙理工大学教授, 博士。

假设转子因初始不平衡引起的偏心点为 A (见图 2), 引起的动挠度为 y_0 , A 所在的径向方向和 y_0 所在的径向方向的夹角为 θ 。动挠度 y_0 使转子在 H 点产生剧烈摩擦, 从而使转轴在 y_0 方向产生摩擦热弯曲, 在 y_0 方向的热弯曲偏心点为 B 。原始偏心与摩擦热弯曲的合成偏心点为 C 。新的偏心 C 将导致新的动挠度 y_1 , 产生新的摩擦热弯曲偏心点 B_1 。这种循环在某些条件下继续进行下去, 使得转子的摩擦振动呈现波动变化的特征^[5]。

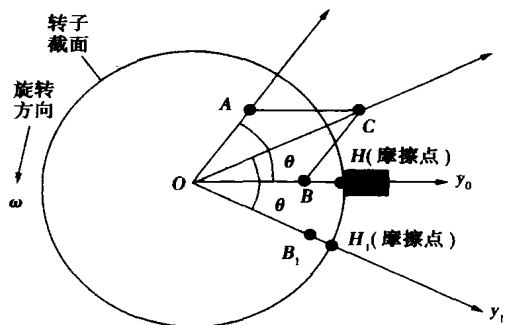


图 2 摩擦引起的热不平衡

3 不同转速的转子摩擦振动行为分析

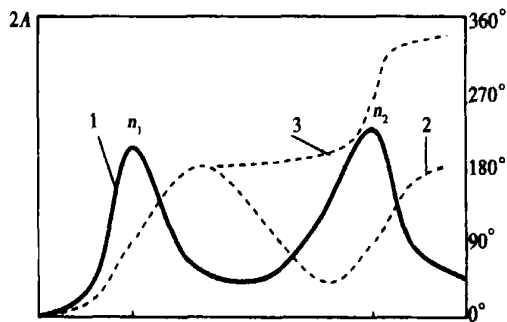
由式(4)可知, 激振力与激振力引起的动挠度之间的夹角 θ 和频率比 γ 及阻尼比 ζ 有关。在机组阻尼变化较小的情况下, 振动幅值和相位角 θ 与频率比 γ 有明显的关系。根据转子工作转速的不同, 将转子分为刚性转子和柔性转子。刚性转子和柔性转子的振动特性有较大的差异。

3.1 刚性转子的摩擦振动行为分析

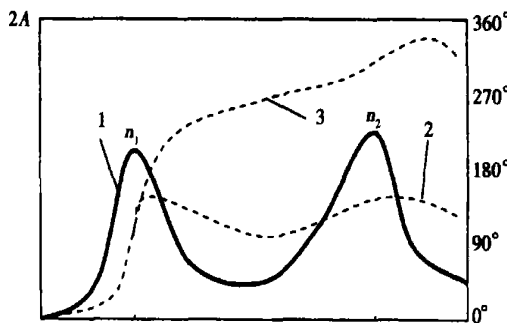
在转子动力学领域, 当转子的工作转速小于第一阶临界转速时的转子定义为刚性转子。在转子静止时, 即 $\omega=0$ 的情况下, $\gamma=0$, 此时式(3)中分子为零, 所以 $\theta=0$ 。在转子的转速 $\omega \ll \omega_k$ 时, $\gamma \approx 0$, 故 $\theta \approx 0$ 。这就意味着原始不平衡的偏心质量方向与其引起的动挠度方向基本一致, 同时使摩擦热弯曲的方向与原始不平衡的偏心质量方向基本一致。在这种情况下, 由于摩擦热弯曲引起的振动矢量与原始振动矢量的方向基本一致, 从而使转子的振动不断加剧, 最终导致转子永久弯曲, 甚至机组被破坏。刚性转子的碰磨振动会发生幅值波动, 相位角逆转向旋转。

3.2 柔性转子的摩擦振动行为分析

当转子的工作转速接近或大于第一阶临界转速时称为柔性转子。柔性转子的幅—频特性和相—频特性见图 3。



(a) 一阶和二阶不平衡分布在同一平面内



(b) 一阶和二阶不平衡分布相互垂直

1—振幅转速特性; 2, 3—转子两端振动相位转速特性

图 3 由一阶和二阶不平衡分布合成的不平转子幅相特性

若转子的转速在第一阶临界转速附近, 即 $\omega \approx \omega_k$, 则 $\gamma \approx 1$, 故 $\theta \approx \pi/2$ 。这就意味着原始不平衡的偏心质量方向与其引起的动挠度方向相差 90° , 摩擦热弯曲的方向与原始不平衡的偏心质量方向相差 90° , 合成振动随时间发生波动, 振动相位逆转向旋转。

若转子的转速介于 $\omega_{n1} \sim \omega_{n2}$ 之间, 则转子的摩擦振动特性比较复杂。对于图 3 所示的两种不平衡分布情况: (1) 一阶不平衡分布与二阶不平衡分布同一平面时, 若在转子中部发生碰磨, 则使转子产生弓形弯曲, 热弯曲方向与一阶不平衡离心力之间相差大约 180° , 此时的摩擦振动不发散。若在靠近转子端部(如汽轮机的轴封处, 或在发电机转子的密封瓦处)位置发生碰磨, 则会激起二阶不平衡响应; 当转速接近 ω_{n2} 时, 原始不平衡响应的幅值显著增加, 摩擦振动响应与原始不平衡引起的振动响应相差 90° 或 180° , 合成振动的幅值增加, 将激起剧烈的摩擦振动响应, 振动且将随时间发生波动, 其中一端

(机械滞后角小于 180°) 振动相位逆转向旋转, 另一端(机械滞后角大于 180°) 振动相位顺转向旋转。
 (2) 一阶不平衡分布与二阶不平衡分布成 90° 时, 不管在什么部位发生碰磨, 都会产生随时间波动的摩擦振动, 特别是当转速接近 ω_{n2} 时, 原始不平衡响应的幅值显著增加, 将激起剧烈的摩擦振动响应, 其中一端(机械滞后角小于 180°) 振动相位逆转向旋转, 另一端(机械滞后角大于 180°) 振动相位顺转向旋转。

若转子的转速大于 ω_{n2} 且在其附近时, 在转轴中部碰磨不会激起发散的摩擦振动; 若在靠近转子端部位置发生碰磨, 则会激起二阶不平衡响应。对于图 3 所示的两种不平衡分布情况: (1) 一阶不平衡分布与二阶不平衡分布在同一平面时, 在转子的一端(机械滞后角接近 180°) 发生的碰磨振动是收敛的, 而在另一端(机械滞后角接近 360°) 发生的碰磨振动是发散的。(2) 一阶不平衡分布与二阶不平衡分布成 90° 时, 在任何一端发生的碰磨都将激起不稳定摩擦振动, 其中一端(机械滞后角小于 180°) 振动相位逆转向旋转, 另一端(机械滞后角大于 180°) 振动相位顺转向旋转。

4 旋转机械转子动静摩擦点轴向位置识别

方法

由前面的分析可知, 不稳定摩擦振动的主要特征是振幅波动, 振动相位逆转向或顺转向旋转。这种现象的本质就是, 在转轴表面发生碰磨时, 合成振动矢量发生旋转。因此, 可以利用振动矢量的变化关系来实现碰磨点的轴向定位。

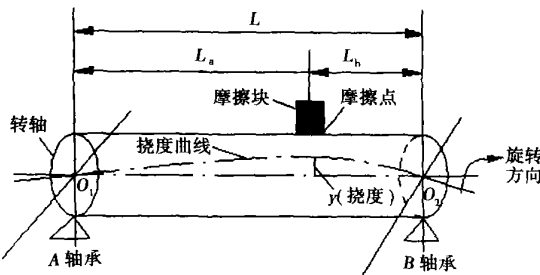


图 4 摩擦点轴向定位示意图

设一根转轴两端轴承(A 和 B)的轴向距离为 L (见图 4)。摩擦点与轴承 A 和 B 的距离分别为 L_a 和 L_b 。转轴在初始不平衡力的作用下产生的动挠度为 y , 其为一连续曲线。设原始不平衡在 A 轴承

和 B 轴承引起的振动分别为 X_{A0} 和 X_{B0} , 由于摩擦使转子产生热弯曲, 致使转子在 A 轴承和 B 轴承产生新的合成振动, 分别 X_{A1} 和 X_{B1} 。摩擦热弯曲在 A 轴承和 B 轴承上产生的振动分别为 X_A 和 X_B , 则:

$$\begin{cases} X_A = X_{A1} - X_{A0} \\ X_B = X_{B1} - X_{B0} \end{cases} \quad (5)$$

当转子的摩擦热弯曲变形量很小、振动的幅值很小的情况下, 振动力与其产生的位移之间满足线性关系, 即振动位移的大小正比于振动激振力的大小。而摩擦热弯曲产生的激振力分解到两个轴承座上后, 得到的分力分别为 F_A 和 F_B , 则:

$$\begin{cases} |F_A| = \frac{L_b}{L_a + L_b} |F| \\ |F_B| = \frac{L_a}{L_a + L_b} |F| \end{cases} \quad (6)$$

式中: F —摩擦热弯曲产生的离心力。而:

$$\begin{cases} |X_A| = \frac{1}{K_{da}} |F_A| \\ |X_B| = \frac{1}{K_{db}} |F_B| \end{cases} \quad (7)$$

式中: K_{da} 和 K_{db} 分别为 A 轴承座和 B 轴承座的动刚度。在转子两端轴承动刚度特性一致的情况下, $K_{da} = K_{db}$ 。所以, 摩擦点的轴向位置可用下式来确定:

$$\frac{L_a}{L_b} = \frac{|X_B|}{|X_A|} \quad (8)$$

即:

$$L_a = \frac{|X_B|}{|X_A| + |X_B|} \times L \quad (9)$$

5 摩擦故障轴向定位的现场测试与信号分

析方法

为了确定碰磨点在转子的轴向位置, 选择该转子的两端轴承安装传感器。两个轴承处传感器的安装方向应相互对应。每两个相互对应的传感器信号为一组, 至少应有两组传感器。信号的检测与处理过程见图 5。

利用位移传感器采集转轴的振动位移通频信号, 所采集的通频信号经前置放大后进入 A/D 转换, 再进行数字滤波, 经快速 FFT 后, 提取振动信号的工频振动矢量, 然后将当前工频振动矢量与从历史数据库中调出的工频振动矢量进行比较计算, 得出摩擦引起得振动变化量的大小, 从而确定摩擦点的位置。

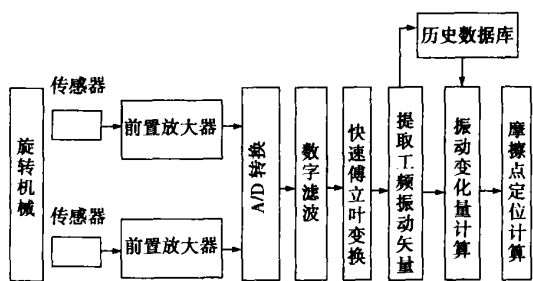


图5 摩擦点轴向定位的信号检测与处理过程示意图

6 动静碰磨故障定位研究实例

国内某发电厂4号汽轮机组是引进美国西屋公司技术生产的N300—16.7/537/537亚临界、中间再热、单轴、双缸双排汽、凝汽式汽轮机。该机组在新机安装调试期间轴系振动超标,发生了转子摩擦弯轴及轴系与轴子不平衡引起的振动现象。该机组首次启动过程中,按正常开机顺序升速至2040 r/min暖机,机组振动正常,1号和2号瓦振动为49.9 μm $\angle 44^\circ$ 和29.3 μm $\angle 106^\circ$ 。但随后1号和2号瓦振动开始爬升,90 min后,1号和2号瓦振动达108 μm $\angle 44^\circ$ 和60.9 μm $\angle 69^\circ$ 。下面用本文提出的方法判断摩擦点的轴向位置。

由式(5)可得:

$$\begin{aligned} \bar{X}_A &= \bar{X}_{A1} - \bar{X}_{A0} \\ &= 108 \angle 44^\circ - 49.9 \angle 44^\circ = 58.1 \mu\text{m} \angle 44^\circ \end{aligned}$$

$$\begin{aligned} \bar{X}_B &= \bar{X}_{B1} - \bar{X}_{B0} \\ &= 60.9 \angle 69^\circ - 29.3 \angle 106^\circ = 41.4 \mu\text{m} \angle 43.8^\circ \end{aligned}$$

由式(9)得: $L_a = 0.42L$ 。也就是说,碰磨的位置发生在高中压转子中部的稍微偏1号轴承的位置上。根据实际检查的结果,实际碰磨位置与本文的分析判断结果基本一致。

参考文献:

- [1] 张善鹏,周广顺.汽轮发电机组转子碰磨振动的理论分析及实例[J].动力工程,2003,23(6):2850-2854.
- [2] 陆颂元,童小忠.汽轮机现场动静碰磨故障的振动特征及分析诊断方法[J].动力工程,2002,22(6):2020-2024.
- [3] 钟一谭,何衍宗,王正,等.转子动力学[M].北京:清华大学出版社,1987.
- [4] 伽西R,菲茨耐H.转子动力学导论[M].北京:机械工业出版社,1986.
- [5] 李录平.汽轮机故障诊断技术[M].北京:中国电力出版社,2002.

(渠源 编辑)

技术改进

GE公司2007年将推出功率加大的50 Hz 109H机组

据《Gas Turbine World》2005年7~8月号报道,GE Energy已经优化了其闭路蒸汽冷却50 Hz 109H联合循环装置的设计,以便使其输出功率从480 MW增加到520 MW。

应用于原型9H燃气轮机升级改造的关键设计技术包括:

(1)燃料加湿

应用专利技术,给燃料(天然气)加湿,以便增加通过涡轮的质量流量,同样数量的燃料将产生更多的输出功率,同时也减少了有害物排放。

(2)优化间隙控制

根据系统的运行,重新配置了主动间隙控制系统,以便为前两个涡轮级提供优化的间隙。

(3)冷却和密封的改进

根据实际的运行温度,调节冷却空气流量到临界的流量,GE精细调整原冷却设计,优化性能,提高零件寿命。燃气初温将继续保持在1400 $^\circ\text{C}$,在进一步优化涡轮设计,可取得低于预期的第一级温降。

功率加大的520 MW、60%效率的H技术机组在商业上是实用的,并在2007年初即可交付使用。

在2007年按计划的热燃气通路检查期间,许多新的设计特点将作为改进项目在巴格兰湾处的现有机组上应用。

(吉桂明 供稿)

cle analyzed is the impact of such parameters as turbine entry temperature, pressure ratio, injection ratio and regeneration ratio, etc on cycle efficiency and specific work. Through a comparison and discussion of the specific features of the two relevant cycles the authors have come to the conclusion that the humid air injected cycle makes it possible to enhance output power by 10% ~ 25%, reduce heat consumption rate by 6% ~ 15% and NO_x emissions by 15% ~ 50%. Moreover, the above-mentioned modification can be implemented on existing power plants. **Key words:** gas turbine, steam injected gas turbine, regenerative gas turbine, humid air cycle

火电机组轴封渗漏及利用系统的通用计算方法 = **A General Method for Calculating the Shaft Seal Leakage and Utilization System of a Thermal Power Plant** [刊, 汉] / CHEN Hai-ping, YU Shu-mei, ZHANG Shu-fang (Power Engineering Department, North China University of Electric Power, Baoding, China, Post Code: 071003), SHI Wei-zhu (Beifang United Electric Power Co., Huhuohaote, Inner Mongolia, China, Post Code: 010020) // Journal of Engineering for Thermal Energy & Power. — 2006, 21(1). — 19 ~ 21, 26

With the shaft seal leakage and utilization system of a thermal power plant serving as an object of study and on the basis of a comprehensive consideration of its system configuration and composition features deduced was a model of quantitative analytic calculations for the shaft seal leakage and utilization system. This model adopts a matrix-form expression with the presence of a one-to-one correspondence between the calculation model and the thermal system configuration. Its usage features simplicity and conciseness in calculations and high versatility. The model can be used for the analysis of power units of various types and different operating conditions, and is especially suited to serve as a computer processing-based mathematical model. In view of the above the model under discussion is of major theoretical significance for the realization of energy-savings and the reduction in energy consumption for thermal power plants. **Key words:** thermo-economics, shaft seal leakage and utilization system, general calculation method, thermal system, matrix

低温多效蒸馏海水淡水—发电联产系统经济性分析 = **An Analysis of the Cost-effectiveness of a Cogeneration System for the Simultaneous Production of Electric Power and also Fresh Water by Low-temperature Multi-effect Distillation of Seawater** [刊, 汉] / SHEN Sheng-qiang, YANG Luo-peng (Department of Power Engineering, Dalian University of Science & Technology, Dalian, China, Post Code: 116024) // Journal of Engineering for Thermal Energy & Power. — 2006, 21(1). — 22 ~ 26

With respect to a cogeneration system for the simultaneous production of electric power and also fresh water by low-temperature multi-effect distillation of seawater the energy cost of water-making and the impact of extracted-steam heating on a steam turbine unit were calculated using an equivalent enthalpy drop theory. In conjunction with a $q-\gamma-\tau$ matrix equation constructed were a partial quantitative analytic matrix model and an equivalent enthalpy drop method-based steam-extraction efficiency matrix model featuring high versatility and precision as well as ease of sequencing. By employing the above matrix models it is possible to conveniently, rapidly and accurately calculate water-making power consumption rate and the variation of water-making fuel cost caused by a change in steam extraction pressure and steam heating temperature. The results of the calculation indicate that compared with the traditional performance index water-making ratio or gained output ratio (GOR) the use of water-making electric power consumption rate can more accurately evaluate the thermal performance of the water-electricity cogeneration system. The reduction of steam extraction pressure and steam heating temperature is favorable to lowering the water-making energy cost. However, the lower limit of steam extraction pressure and steam heating temperature should respectively meet the requirements of ejection factor of steam injector and compression ratio. The cogeneration system for the simultaneous production of electric power and also fresh water by low-temperature multi-effect distillation of seawater can effectively resolve the water shortage problem in northern China coastal areas, especially that of thermal power plants in those areas. **Key words:** equivalent enthalpy drop, cogeneration of water and electricity, low-temperature multi-effect distillation, seawater desalination

基于矢量分析的转子碰磨故障轴向定位方法 = **Vector Analysis-based Axial Locating Method for Rotor Contact-rubbing Faults** [刊, 汉] / LI Lu-ping, ZOU Xin-yuan, JIN Feng-hua (Institute of Energy Source & Power Engi-

neering under the Changsha University of Science & Technology, Changsha, China, Post Code: 410076) //Journal of Engineering for Thermal Energy & Power. — 2006, 21(1). — 27 ~ 30

On the basis of studying the contact-rubbing vibration behavior of a rotating machine rotor an axial locating method for a rotor contact-rubbing point was explored, and a vibration vector analysis-based axial locating method for a contact-rubbing fault put forward. The results of the study indicate that the contact-rubbing of a rotating shaft surface with some portion of a stator will lead to a temporary thermal bending of the rotor, thus giving rise to a change in non-equilibrium state of the rotor. This change can be reflected through a change in vibration vector at the two ends of the rotor. By utilizing the variation relation of the vibration vector at the two ends of the rotor it is possible to ascertain the axial location of the contact-rubbing point at the rotor surface. The analysis of a practical usage case has shown that the method of locating the contact-rubbing fault of a rotating machine as proposed by the authors possesses adequate precision. **Key words:** rotating machine, contact rubbing, fault locating

基于汽包寿命的 1021 t/h 锅炉启动过程的优化研究 = A Study of the Optimization of a 1021 t/h Boiler Start-up Process on the Basis of the Boiler Drum Service Life [刊, 汉] / GUAN De-qing, MO Jiang-chun, LU Li-ming (Institute of Power & Mechanical Engineering under the Changsha University of Science & Technology, Changsha, China, Post Code: 410076), MAO Yong-zhong (Hunan Provincial Shimen Power Plant, Shimen, Hunan Province, China, Post Code: 415300) //Journal of Engineering for Thermal Energy & Power. — 2006, 21(1). — 31 ~ 34, 38

By using a three-dimensional finite element theory calculated was the stress field of a 1021 t/h boiler drum under the action of an internal pressure. The theoretical stress concentration factor thus obtained is greater than the recommended value of German TRD301 standard by 22.7%. In addition, the thermal stress of the boiler drum under a quasi-steady state was calculated using the theory of thermal elasticity. By employing TRD301 standard the fatigue life of the boiler drum was calculated. With the time step experienced by the pressure-rise range at various stages serving as an optimized parameter, thereby achieving the dual target of lowering fatigue life loss and shortening start-up time, a model of boiler start-up process optimization was set up based on the boiler drum service life. Through calculations optimized curves were obtained for the 1021 t/h boiler cold-state and hot-state start-up process. On this basis, the practical operation of a 1021 t/h boiler for a 300 MW unit at a certain power plant has brought about satisfactory results. A start-up on the basis of these optimized curves can not only ensure a small loss of boiler drum service life, but also significantly shorten boiler start-up time. The optimized start-up curves set up by the authors can provide significant guidance for the boiler operation of the 300 MW plant. **Key words:** boiler drum, fatigue life, start-up process, optimization

W 型火焰锅炉炉膛温度场的可视化试验研究 = Experimental Research on the Visualization of Temperature Fields in a Boiler Furnace with a W-shaped Flame [刊, 汉] / YAO Bin, JIANG Zhi-wei, ZHOU Huai-chun, et al (State Key Laboratory on Coal Combustion under the Huazhong University of Science & Technology, Wuhan, China, Post Code: 430074) //Journal of Engineering for Thermal Energy & Power. — 2006, 21(1). — 35 ~ 38

A flame radiation-image detection system is used to detect the radiation energy emitted from a furnace space to the various image elements of a lens. Then, from the standpoint of energy transmission and equilibrium a spatial temperature field is reconstructed from the obtained images. A visualization reconstruction test for a furnace two-dimensional sectional temperature field was conducted on the W-shaped flame furnace of a 300 MW unit. During the test 4 CCD (charge-coupled device) based flame detectors were installed on the furnace walls and furnace flame radiation images obtained by employing computer image acquisition and processing techniques. Through a processing of the flame radiation images and by using relevant algorithms a temperature distribution of the furnace section was reconstructed. It is possible to dynamically reflect the temperature level of the flame section and also abnormal combustion conditions, such as the deviation of a flame center, a flame brushing past a water wall, etc. The time needed for updating the visualization results of furnace-section temperature field will not exceed 5 seconds, thus adequately meeting the requirements of real-time monitoring. **Key words:** furnace, radiation image formation, furnace section, temperature field, reconstruction